

# Optimal fenestration of the Fontan circulation

Report by Zan Ahmad

Advised by Charles Puelz and Charles S. Peskin

November 28, 2021

## Abstract

This paper describes a computer model for a surgical intervention called a fenestration, which is used to improve the hemodynamics of the Fontan circulation. The fenestration is a shunt between the systemic and pulmonary veins that increases cardiac output at the expense of a decrease in the arterial oxygen saturation. The compartmental computer model used in this paper simulates both blood flow and oxygen transport. This model is used to demonstrate that an optimal fenestration size exists, which maximizes oxygen delivery to the systemic tissues. Numerical experiments are performed to identify the optimal fenestration cross-sectional area in an effort to maximize oxygen delivery for a given set of parameters by balancing the gain in cardiac output with the loss of oxygen content in the systemic tissues.

## 1 Introduction

Hypoplastic left heart syndrome (HLHS) is a rare congenital heart defect in which the left heart is severely underdeveloped. It is usually accompanied by stenosis or atresia of the mitral valve. Patients with this condition require complex medical and surgical interventions to ensure survival. The typical course of treatment is a sequence of surgeries during the first several years of life, ending with a procedure that establishes an abnormal physiology known as the Fontan circulation. This physiology was conceived in 1971 and is characterized by the systemic organs and lungs in series, as in a normal circulation, and passive blood flow to the lungs [1]. The Fontan circulation is achieved by surgically placing the right ventricle upstream from the systemic organs and connecting the vena cava directly to the pulmonary artery. Refer to Figure (2) for a schematic of the Fontan circulation as well as a normal circulation in Figure (1) for comparison. There are several variations of the Fontan circulation that are either intra- or extra-cardiac, depending on the type of connection established between the systemic veins and pulmonary artery. The models considered in this work apply to either case. This Fontan “connection” directs blood directly from the systemic veins to the lungs for re-oxygenation, completely bypassing the heart.

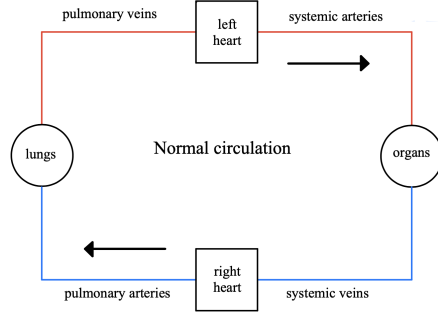


Figure 1: Schematic of the standard postnatal cardiovascular circulation. Oxygenated blood is shown in red and deoxygenated blood is shown in blue. The atrial chambers in this model are grouped with the chambers that precede the respective ventricles.

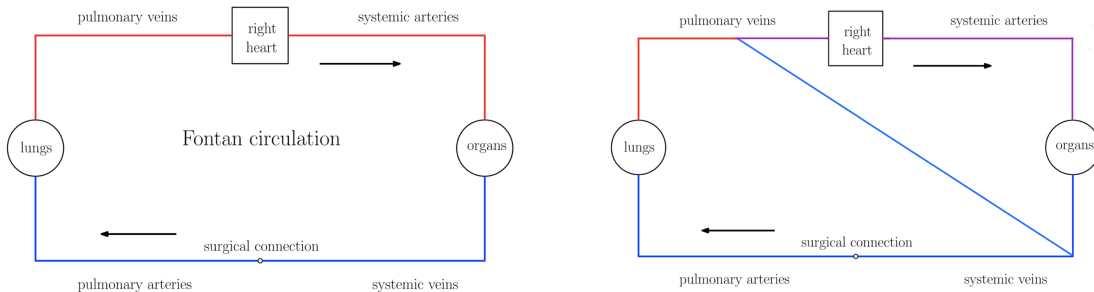


Figure 2: A schematic of the standard Fontan circulation [8] and fenestrated Fontan circulation with a systemic-to-pulmonary shunt. Blue represents deoxygenated blood, red represents oxygenated blood and purple represents partial saturation of oxygen.

Fontan patients experience many complications, like protein-losing enteropathy [6]. These issues might be caused by chronically low cardiac output as a result of high vascular resistance from the serialized systemic organs and lungs. Another possible cause might be weaker contractile properties of the right ventricle [2]. Cardiac output in a Fontan circulation can be increased by introducing a connection between the systemic veins and the pulmonary veins known as a fenestration. While this connection typically increases cardiac output, it does so at the expense of oxygen delivered to the systemic tissues. Blood flowing through the fenestration, which bypasses the lungs, is not re-oxygenated. This leads to a decrease in the oxygen saturation in the systemic tissues. This paper is concerned with modeling the effects of a fenestration. Refer to Figure (2). The clinical function of a fenestration is to increase cardiac output and decrease pulmonary arterial pressure [3], however, since a fraction of the oxygen-poor blood is being directed away from the lungs, the overall oxygen content in the blood is decreased. In this paper, we use a pulsatile mathematical model of the fenestrated Fontan physiology to identify the fenestration which balances the decrease in systemic oxygen saturation with the increase in cardiac output.

## 2 Mathematical Models

Our models for the Fontan circulation are compartmental in nature and contain three main parts: pulsatile blood flow, oxygen transport, and a nonlinear fluid-mechanical resistance to describe the fenestration. The derivation of the pulsatile blood flow model is presented in the first subsection. This is followed by a description of the oxygen transport model. The final subsection details how the size of the fenestration is incorporated into the blood flow and oxygen transport models.

### 2.1 Pulsatile Blood Flow Model

The pulsatile blood flow model takes into account the temporal variations of pressure, flow, and volume by incorporating a time-varying compliance for the heart chambers over a cardiac cycle. Derivations presented herein follow the approach from Hoppenstadt and Peskin, with modifications to account for the Fontan physiology. [4].

The compartmental blood flow models used in this paper contain compliance chambers and resistor elements. The major vessel networks, i.e. the systemic arteries (sa), systemic veins (sv), pulmonary arteries (pa), and pulmonary veins (pv), are taken to be compliance chambers that obey the following relation between compliance  $C$ , pressure  $P$ , and volume  $V$ :

$$V = V_d + CP. \quad (1)$$

The dead volume  $V_d$  is the residual volume of the compliance chamber at zero pressure. The heart chambers obey equation (1), but the compliance is taken to be a time-dependent function that varies between minimum  $C_{\text{systole}}$  and maximum  $C_{\text{diastole}}$ .

The resistor elements in our models determine the connections, and hence the flows, between compliance chambers. For example, flow between chamber  $i$  and chamber  $j$ , denoted  $Q_{ij}$ , is determined by the respective chamber pressures  $P_i$  and  $P_j$  and the resistance  $R$  of the resistor element via Ohm's law:

$$Q_{ij} = R^{-1}(P_i - P_j). \quad (2)$$

Equations (1) and (2) are the building blocks for the hemodynamics in the pulsatile model.

The heart pumps blood into the arteries in discrete surges during contractions, causing the blood pressure to rise and fall periodically. Therefore, in this model, the pressures, flows, and volumes are taken to be time-dependent. Consider a compliance vessel with values for inflow  $Q_1(t)$  and outflow  $Q_2(t)$ . If the vessel is not in a steady state, then these two values are unequal and the volume of the vessel is no longer a constant. Let the volume of a vessel be regarded as  $V(t)$  at a time  $t$ . We say the rate of change of volume with respect to time is the difference between the inflow and outflow of the vessel:

$$\frac{dV}{dt} = Q_1 - Q_2. \quad (3)$$

The compliance equation (1) can be used to relate volume as so:

$$V(t) = CP(t) + V_d. \quad (4)$$

Deriving this equation with respect to time yields the equality:

$$C \frac{dP}{dt} = Q_1 - Q_2, \quad (5)$$

a convenient differential equation that accounts for pressure as a function of time in a compliance chamber with unsteady flow.

Consider an arbitrary collection of  $N$  compliance chambers. Between any pair  $i, j \in \{1, 2, \dots, N\}$  we assume there are two resistance vessels that run between them equipped with valves. Connections between chambers that are not present in the circulation can be ignored by making the resistance between them infinite in both direction. If there is a connection between two chambers with no valve, this can be achieved in the model by setting two resistances between them in both directions to be equal and finite. Finally, if there is a connection between two chambers with a valve in place to prevent back-flow in a particular direction, we set the resistance in one direction to be infinite and the resistance in the direction of flow to be a small finite value. By choosing the right combination of resistances, any circulation set up may be achieved, including the fenestrated Fontan circulation.

The equation for the conservation of volume for each compliance chamber follows the same form as before where the change in volume with respect to time is the difference between the inflow and the outflow:

$$\frac{dV_i}{dt} = \sum_{j=1}^N (Q_{ji} - Q_{ij}), i = 1, \dots, N. \quad (6)$$

where  $V_i$  is the volume of the  $i$ th compliance chamber and  $Q_{ij}$  is the flow from chamber  $i$  to chamber  $j$ .

The compliance relation is given by:

$$V_i = V_{d,i} + C_i P_i \quad (7)$$

where  $C_i$  and  $P_i$  are the compliance and pressure of the  $i$ th compliance chamber respectively, and  $V_{d,i}$  is the dead volume or volume at  $P_i = 0$  of the  $i$ th compliance chamber. For arteries and veins the compliance is constant and for chambers of the heart it is a function of time. Specifically, we take the right ventricular compliance  $C_{RV}$  to be a given periodic function of time with period  $T$  and express it in a way that considers time  $t = 0$  to be at end-diastole and thus at a maximum compliance,  $C_{RVD}$ , and time  $t = T$  to be at end-systole and thus at a minimum compliance  $C_{RVS}$ . We introduce the quality of the ventricle called elastance,  $E$ , which is the reciprocal of compliance, and specify ventricular qualities in terms of maximum and minimum elastance [7]:

$$E_{\max} = 1/C_{RVS} \quad (8)$$

$$E_{\min} = 1/C_{RVD} \quad (9)$$

The time dependent equation for compliance in the right ventricle in terms of elastance is given by

$$C_{RV}(t) = \frac{1}{E_{RV}(t)} \quad (10)$$

$$E_{RV}(t) = k \frac{g_1}{1 + g_1} \cdot \frac{1}{1 + g_2} + E_{\min} \quad (11)$$

where

$$g_1 = \left(\frac{t}{\tau_1}\right)^{m_1}, \quad g_2 = \left(\frac{t}{\tau_2}\right)^{m_2} \quad (12)$$

and  $k$  is a scaling factor that guarantees that  $\max(E) = E_{\max}$ , as follows:

$$k = \frac{E_{\max} - E_{\min}}{\max\left[\left(\frac{g_1}{1+g_1}\right), \left(\frac{1}{1+g_2}\right)\right]} \quad (13)$$

In the above expressions, also known as the two-Hill function, the repeating qualitative characteristics of periodic contraction/stiffening and relaxation of the ventricular muscles is quantitatively incorporated into the model, with the systolic and diastolic time constants  $\tau_1$  and  $\tau_2$  inversely controlling the time translation between these extrema and the systolic and diastolic rate constant  $m_1$  and  $m_2$  controlling the slope for these transitions.

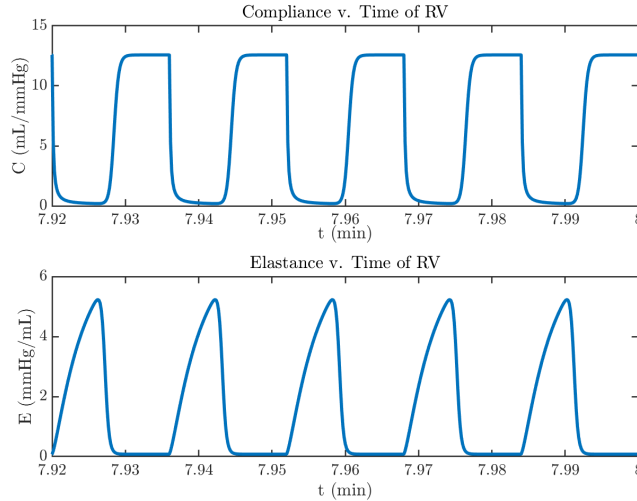


Figure 3: The compliance and elastance reciprocal as a function of time are shown here for 5 cardiac cycles. The peaks (troughs) of the elastance curve and the troughs (peaks) of the compliance curve represent the systolic (diastolic) phase.

The pressure-flow relation for each component is given by entry  $i$  of  $N \times 1$  pressure  $P$  and compliance  $C$  arrays and entry  $(i, j)$  of an  $N \times N$  conductance matrix,  $G$ , equipped with a valve indicator function incorporated into Ohm's Law:

$$Q_{ij} = \frac{\mathbf{1}_{ij}}{R_{ij}}(P_i - P_j) = \mathbf{1}_{ij}G_{ij}(P_i - P_j), i, j = 1, \dots, N, \quad (14)$$

where we define an  $N \times N$  indicator matrix with entries in position  $ij$  by:

$$\mathbf{1}_{ij} = \begin{cases} 0 & P_i \leq P_j \\ 1 & P_i > P_j \end{cases} \quad (15)$$

and the notation  $G_{ij} = 1/R_{ij}$  is introduced so we may refer to an infinite resistance as zero conductance. Combining volume conservation equations with the compliance relations gives:

$$\begin{aligned} \frac{d}{dt}(C_i P_i) &= \sum_{j=1}^N (\mathbf{1}_{ji} G_{ji} (P_j - P_i) - \mathbf{1}_{ij} G_{ij} (P_i - P_j)) \\ &= \sum_{j=1}^N (\mathbf{1}_{ij} G_{ij} + \mathbf{1}_{ji} G_{ji}) (P_j - P_i) \end{aligned} \quad (16)$$

In our model, the systemic organs and pulmonary circulation are assumed to be resistance elements, with resistances  $R_s$  and  $R_p$  respectively. The fenestration and Fontan connection are also assumed to be resistance elements with resistance  $R_{Fe}$  and  $R_{Fo}$  respectively.

## 2.2 Oxygen Model

An important consideration for congenital heart defects such as hypo-plastic left heart syndrome and other single ventricular circulations is the oxygen content, since the normal distribution of oxygen concentration in the blood across the compliance chambers is interrupted by the modifications, and in our case, even further with the introduction of the fenestration. The shunt we incorporate into our model connects the systemic vein compliance chamber to the pulmonary vein compliance chamber. What this means is that some of the blood volume that was originally meant to flow to the lungs to receive oxygen is now bypassing the lungs and is not receiving oxygen, resulting in an overall lower oxygen concentration. We compute this by the following equation:

$$\frac{d}{dt}(V_i [\text{O}_2]_i) = \sum_{\substack{j, j \neq i \\ Q_{ji} > 0}}^N (Q_{ji} [\text{O}_2]_j) - \sum_{\substack{j, j \neq i \\ Q_{ij} > 0}}^N (Q_{ij} [\text{O}_2]_i) - M_{ij} \quad (17)$$

Here we refer to  $[\text{O}_2]_i$  as the volumetric oxygen concentration in the  $i$ th compliance chamber, defined as the volume (in liters) of oxygen per liter of blood, so it is a unit-less quantity. The first summation represents inflow, accounting for oxygen carried by blood flow from chamber  $j$  into chamber  $i$  and the second summation is the outflow, which accounts for oxygen that is carried out of chamber  $i$  by the blood into chamber  $j$ .  $M_{ij}$  is called metabolism, the rate of oxygen consumption in the vessel leading from chamber  $i$  to  $j$ . We consider the lungs to be an oxygen source and the organs to be an oxygen sink, and therefore these are the only places where the metabolism function is nonzero. We give  $M_{sa,sv}$  a positive constant value based on clinical data to model the consumption of oxygen by the organs, and we give  $M_{pa,pv}$  a negative value since the metabolism is intrinsically defined as oxygen consumption and the lungs are delivering oxygen to the blood. In particular, the expression is as follows:

$$M_{pa,pv} = -(Q_p (\gamma - [\text{O}_2]_{pa})) \quad (18)$$

where  $\gamma > 0$  represents the volumetric oxygen concentration of blood when it is fully saturated and  $Q_p$  is the pulmonary flow,  $Q_{pa,pv}$ , or the flow through the lungs.

### 2.3 Geometric Considerations for Fenestration

One of the more useful properties of the fenestration that we can compute is its size. Since the fenestration resistance/conductance is a parameter in our model, we can relate this to the dimensions of the conduit with Gorlin's equation. Consider the systemic veins and the pulmonary veins as two chambers separated by a hole with a cross-sectional area  $A_0$ . We make the assumption that the blood flow's velocity is much greater than the velocity of the blood inside the chambers already and thus we regard the blood in the chambers to be at rest. The flow in the direction of the systemic veins to the pulmonary veins is considered positive. The equation for the velocity of the fluid through the hole as it relates to flow is given by:

$$v = Q/A_0 \quad (19)$$

where  $Q = Q_{sv,pv}$  is the flow through the fenestration.

Let  $P_0$  be the pressure within the fenestration. Then by Bernouli's equation for the chamber upstream of the shunt and up to it:

$$P_0 = P_{sv} - \frac{1}{2}\rho v^2 = P_{sv} - P_{sv} \quad (20)$$

For the chamber downstream of the hole, the pressure in this region is constant such that  $P_{sv} = P_0$  and Bernouli's equation does not apply due to the turbulence of the fluid resulting in dissipation of energy, since Bernouli's principle is derived from conservation of energy. We can use the property of the downstream pressure to state the following:

$$P_{sv} - P_{pv} = \frac{\rho}{2A_0^2}Q^2, Q > 0 \quad (21)$$

$$P_{pv} - P_{sv} = \frac{\rho}{2A_0^2}Q^2, Q < 0 \quad (22)$$

Combining the equations above yields:

$$P_{sv} - P_{pv} = \frac{\rho}{2A_0} |Q| Q \frac{P_{sv} - P_{pv}}{Q} = R_{Fe} \quad (23)$$

We now have an equation for resistance in terms of cross sectional area of the fenestration.

$$R_{Fe} = \frac{\rho}{2A_0} |Q| \quad (24)$$

Of course, since blood is not an ideal fluid, it has some viscosity that contributes to resistance denoted as  $R_{visc}$ :

$$R_{Fe} = R_{visc} + \frac{\rho}{2A_0} |Q| \quad (25)$$

Since the resistance is the reciprocal of the conductance, we can take the reciprocal of both sides to arrive at an equation for conductance in terms of  $Q$  and  $A_0$ :

$$G_{sv,pv} = G_{Fe} = \frac{1}{R_{visc} + \frac{\rho}{2A_0} |Q|} \quad (26)$$

### 3 Numerical Methods

In this section, we show how the equations for the heart model are numerically solved. All the implementations for these simulations are carried out in MATLAB.

#### 3.1 Pulsatile Bloodflow Model

A numerical method for (16) can be obtained by replacing the time derivative with a backward difference quotient, which is known as Backward Euler Method. Since this is a system of  $N$  differential equations with  $N$  unknowns  $P_1, \dots, P_N$ , the backward Euler method can be used to solve:

$$\frac{C_i(t)P_i(t) - C_i(t - \Delta t)P_i(t - \Delta t)}{\Delta t} \quad (27)$$

$$= \sum_{j=1}^N (\mathbf{1}_{ij}(t)G_{ij}(t) + \mathbf{1}_{ji}(t)G_{ji}(t))(P_j - P_i) \quad (28)$$

While the valve states  $\mathbf{1}_{ij}(t)$  are unknown, we regard them as functions of the pressures and consequentially make the assumption that for now they are known values. This allows us to express the equation above as a linear system which we rewrite in standard form:

$$\sum_{j=1}^N A_{ij}(t)P_j(t) = C_i(t - \Delta t)P_i(t - \Delta t), i = 1, \dots, N \quad (29)$$

where

$$A_{ij}(t) = -\Delta t(\mathbf{1}_{ij}(t)G_{ij}(t) + \mathbf{1}_{ji}(t)G_{ji}(t)), i \neq j \quad (30)$$

$$A_{ii}(t) = C_i(t) - \sum_{j:j \neq i} A_{ij}(t). \quad (31)$$

Once we solve for the pressures, we can plug these into Ohm's law (2) to get the flows.

#### 3.2 Oxygen Model

To solve the ODE for the oxygen concentration in each chamber (17), we replace the time derivative with a forward difference quotient to get the explicit numerical integration scheme known as Forward Euler's method:

$$\frac{V_i[\text{O}_2]_i(t) - V_i[\text{O}_2]_i(t - \Delta t)}{\Delta t} = Q_{ji}[\text{O}_2]_j(t - \Delta t) - Q_{ij}[\text{O}_2]_i(t - \Delta t) - M_{ij}(t - \Delta t) \quad (32)$$

It is simple to solve for  $V_i[\text{O}_2]_i(t)$  which we can divide the volume out from to obtain the oxygen concentration at any given time in the simulation.

### 3.3 Gorlin Equation and a Fixed Point Iteration

When the fenestration is closed ( $A_0 = 0$ ), the above formulations will suffice. However, if we are to consider an open fenestration ( $A_0 > 0$ ), we must use the Gorlin equation (26) to solve for the fenestration resistance. Unlike the other resistor elements in the model, the fenestration resistor is a nonlinear element that depends on the flow between chambers it connects. Because of this dependence of the resistance (and conductance) on the flow, we need to ensure that at each timestep, we are using the appropriate flow value,  $Q_{sv,pv}(t)$ , for that time to compute  $G_{Fe} = \frac{1}{R_{Fe}}$  instead of time-lagging with the previous flow value  $Q_{sv,pv}(t - \Delta t)$ . To do this, we implement a fixed-point iteration on  $Q_{sv,pv}(t - \Delta t)$  at each time step to generate a sequence  $\{Q_{sv,pv}(t - \Delta t)\}_k, k = 0, 1, 2, \dots$  which converges to  $Q_{sv,pv}(t - \Delta t)$ , given by

$$\phi(Q_{sv,pv}(t - \Delta t)_k) = Q_{sv,pv}(t - \Delta t)_{k+1} \quad (33)$$

where  $\phi$  is the map that takes a fenestration flow value and uses it to solve for the respective conductance and then in turn uses that updated conductance value to get the flow value that becomes the next iterate in the sequence (33). Just as  $\{Q_{sv,pv}(t - \Delta t)\}_k, k = 0, 1, 2, \dots$  converges to  $Q_{sv,pv}(t - \Delta t)$ , a similar sequence  $\{G_{Fe}(t - \Delta t)\}_k, k = 0, 1, 2, \dots$  is generated and converges to  $G_{Fe}(t)$ . Using the fixed-point iteration on these flows avoids high frequency oscillations and numerical instability in the timecourses.

## 4 Results

In the following simulations, our model runs for roughly 8 minutes which equates to about 500 cardiac cycles. This ensures that both the hemodynamics and the oxygen-related values reach a periodic steady-state.

### 4.1 Closed Fenestration: Standard Fontan Circulation

In this section we consider the results of the simulation prior to the introduction of a fenestration. The values for the various parameters we used in this model are shown here and have been calibrated to be consistent with clinical data found in [5].

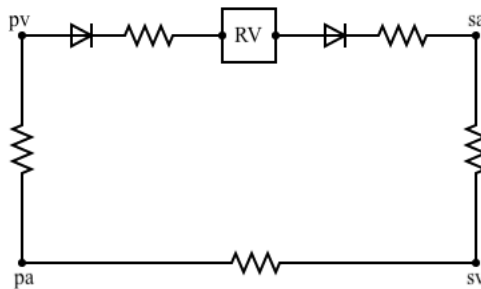


Figure 4: Zero-dimensional bloodflow circuit diagram of the standard Fontan circulation.

### 4.1.1 Parameters and Model Calibration

Parameters	Resistance ( $R$ )	Dead Volume ( $V_d$ )	Compliance ( $C$ )
Units	mmHg/(L/min)	L	L/mmHg
S	20.7807	-	-
P	0.5517	-	-
Ao	0.01	-	-
Tr	0.01	-	-
Fo	0.01	-	-
SA	-	0.705128	7.333e-4
PA	-	0.9303	0.00412
SV	-	2.86885	0.0990
PV	-	0.147541	0.01

Table 1: Parameters for the circulation model. Abbreviations: S, systemic organs; P, lungs; Ao, aortic valve; Tr, tricuspid valve; Fo, Fontan connection; SA, systemic arteries; PA, pulmonary arteries; SV, systemic veins; PV, pulmonary veins.

Parameters	Symbol	Units	Right Ventricle
Minimal elastance	$E_{\min}$	mmHg/L	79.518
Maximal elastance	$E_{\max}$	mmHg/L	5232.0675
Contraction exponent	$m_1$	-	1.32
Relaxation exponent	$m_2$	-	27.4
Systolic time constant	$\tau_1$	minutes	0.269*T
Diastolic time constant	$\tau_2$	minutes	0.452*T
Dead volume	$V_d$	L	0.028
Period of heartbeat	$T$	minutes	0.016

Table 2: Parameters for the time varying right ventricular compliance in the heart model.

The parameters shown above were calibrated to clinical data reported in [5]. The standard Fontan model schematic shown in figure (4) shows that there are two valves in this model represented by diodes. The diode between the chambers labeled pulmonary veins (pv) and the right ventricle (RV) is the tricuspid valve. Note that this is due to the fact that the pulmonary veins are coupled with the right atrium as there is negligible resistance to blood flow between them. The diode between the right ventricle (RV) and systemic arteries (sa) is the aortic valve.

variable	our model	clinical data reported in [5]
cardiac index ( $L \cdot \text{min}^{-1} \cdot \text{m}^{-2}$ )	2.685039	2.9, 2.1
stroke volume index ( $\text{mL} \cdot \text{m}^{-2}$ )	42.97555	39,40
RV end diastolic volume index ( $\text{mL} \cdot \text{m}^{-2}$ )	75.90377	72, 76
RV end systolic volume index ( $\text{mL} \cdot \text{m}^{-2}$ )	32.92821	33, 36
RV end systolic pressure (mmHg)	118.0558	124*
RV end diastolic pressure (mmHg)	6.827076	6.6
vena cava mean pressure (mmHg)	9.348427	8
pulse pressure (mmHg)	56.39481	54
systemic artery systolic pressure (mmHg)	118.0559	124
systemic artery diastolic pressure (mmHg)	61.66108	70
systemic artery mean pressure (mmHg)	93.04392	88
pul artery mean pressure (mmHg)	9.308135	9

Table 3: Calibrated variables from our prefenestration model compared to those extracted from clinical data. The normalization that occurs in the first four variables assumes a body surface area of  $1.5\text{m}^2$ . \*While clinical data is not available for RV end systolic pressure, due to the configuration of the circulation our model makes the assumption that the value should be the same as the systemic artery systolic pressure.

#### 4.1.2 Closed Fenestration Hemodynamics

Here we show the hemodynamic results of the closed fenestration model and justify that blood flow has reached a periodic steady-state.

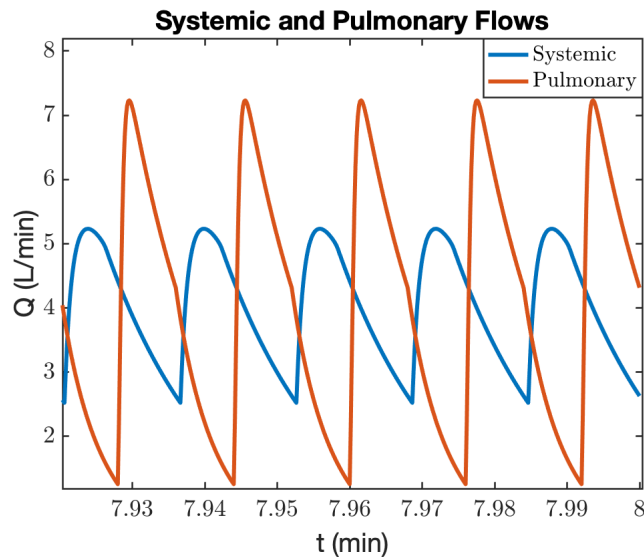


Figure 5: Flow through the organs (systemic) and lungs (pulmonary) for the last 5 cardiac cycles of the simulation.

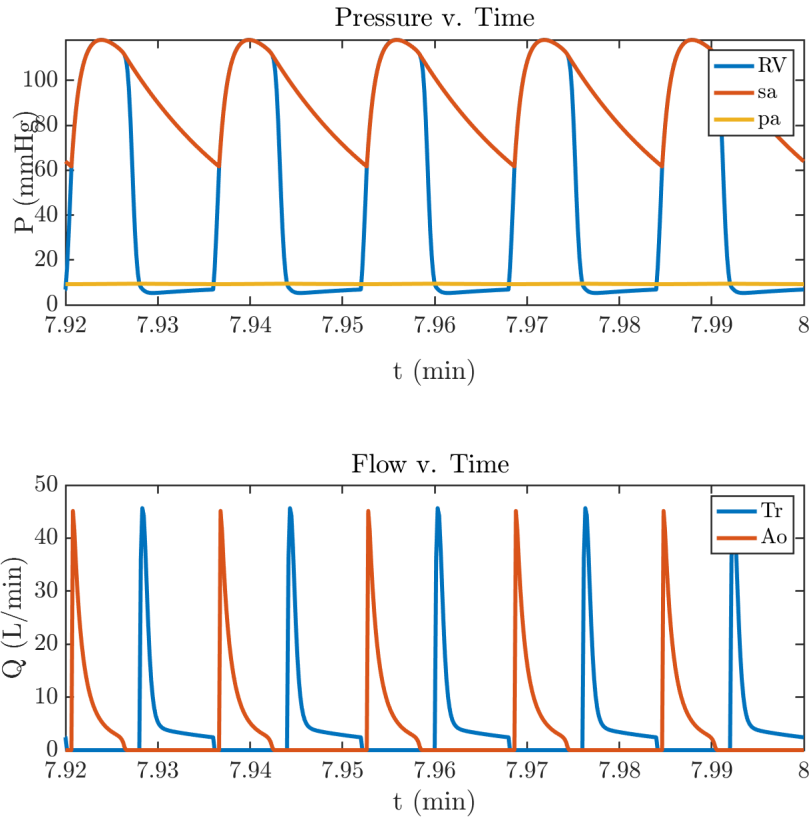


Figure 6: In the first panel, the pressures of the right ventricle, system arteries and pulmonary arteries are shown and in the second panel, the flow through the tricuspid and aortic valves are shown both for the last 5 cardiac cycles of the simulation.

The simulation results in figure 6 demonstrates the connectivity of the Fontan circulation. The right ventricle and the systemic arteries feel the same maximum pressures at the same time because they are conjoined in this physiology. The tricuspid and aortic valves are inversely reaching their maximum and minimum flow values because the tricuspid valve opens to allow the right ventricle to fill. Once the filling process is complete, the tricuspid valve closes and the aortic valve opens in preparation for the ventricle to contract and eject its contents into the systemic arterial tree.

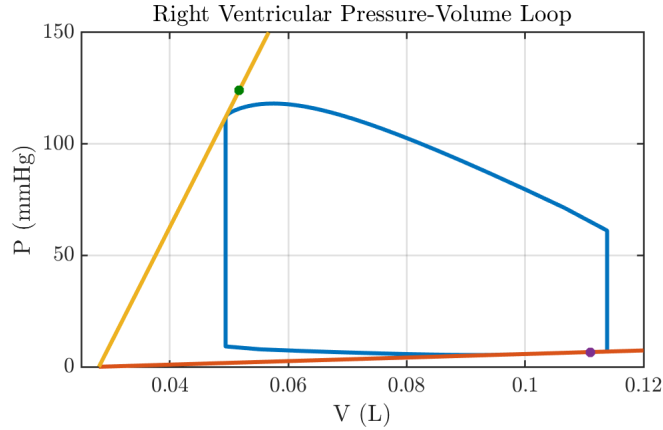


Figure 7: The pressure volume loop for the right ventricle in the last cardiac cycle of the simulation. The points representing the clinical data values of systole and diastole in [5] are shown in green and purple respectively. The intercept of both the yellow and red line is  $V_{RVd}$  and the slopes are  $E_{max}$  and  $E_{min}$  respectively.

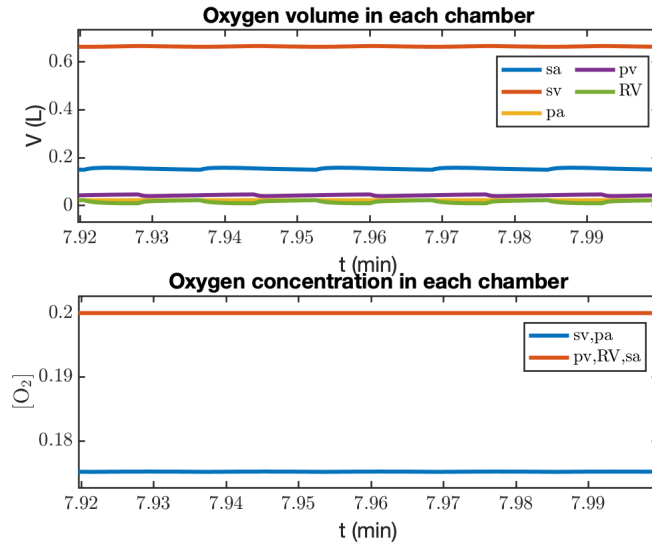


Figure 8: The first panel shows oxygen volume in each respective chamber and the second panel shows the volumetric oxygen concentration, measured as liters of oxygen per liter of blood, in each chamber for five cardiac cycles at the end of the simulation.

## 4.2 Fenestrated Fontan Circulation

In this section we observe the hemodynamical changes that result from the addition of different sized fenestrations.

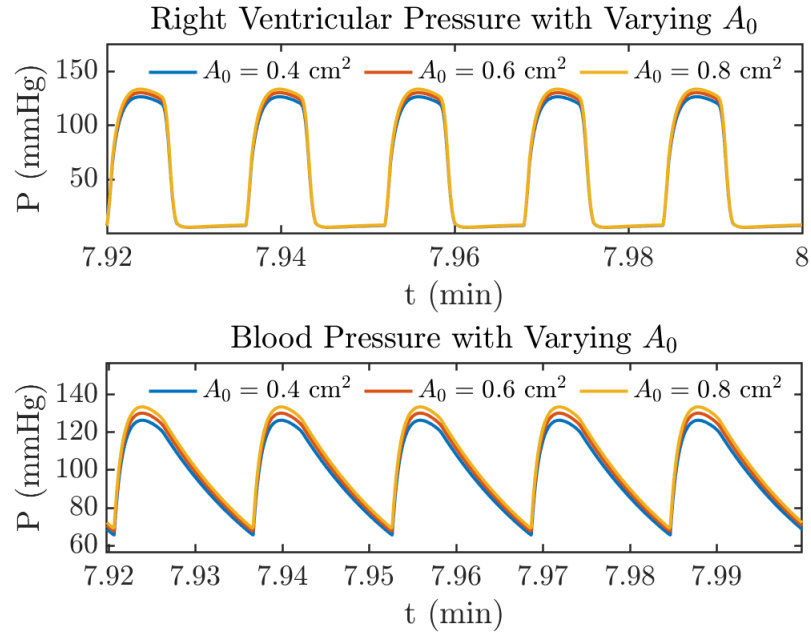


Figure 9: Pressure waveforms over five cardiac cycles for three different fenestration sizes.

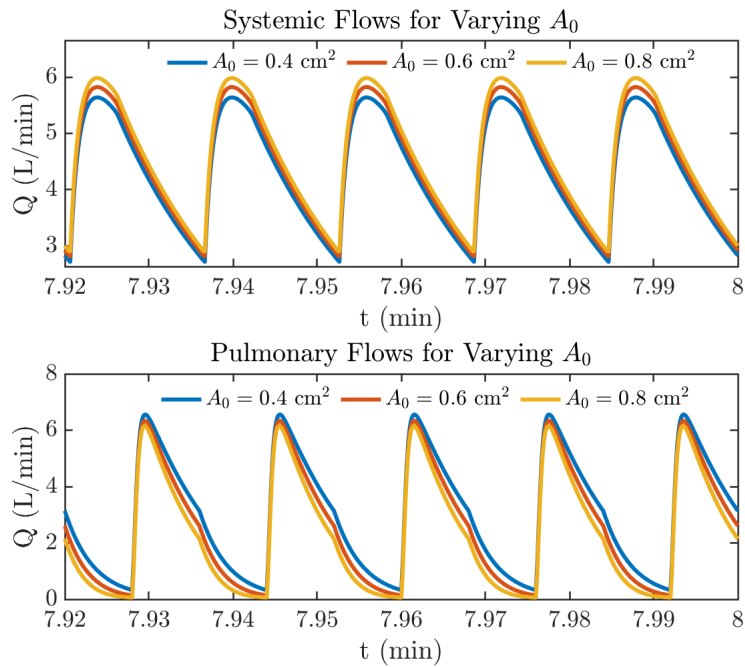


Figure 10: Systemic and pulmonary flows for varying fenestration sizes.

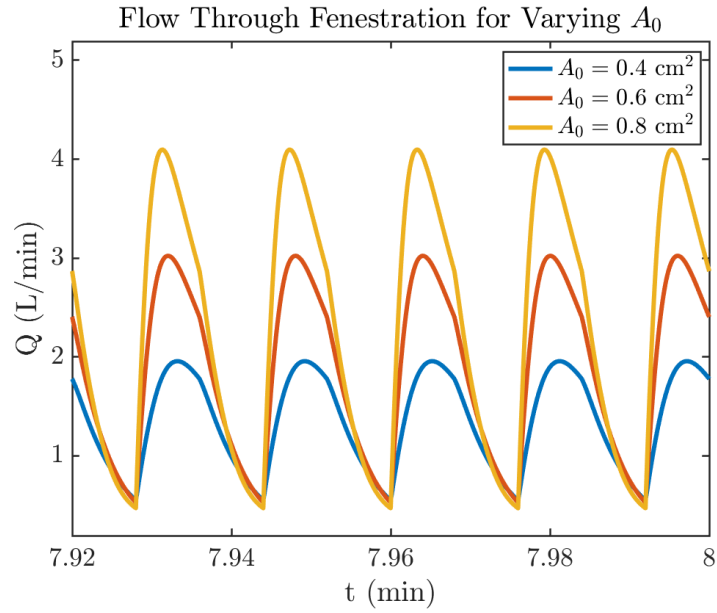


Figure 11: Flow through fenestrations of varying cross-sectional areas in the last five cardiac cycles of the simulation.

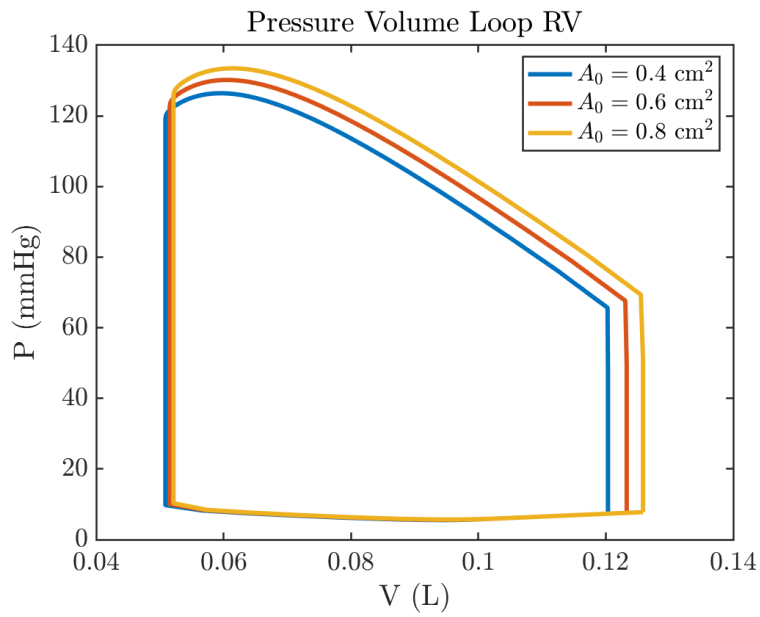


Figure 12: Right ventricular pressure and volume plotted for varying fenestration cross-sectional areas.

### 4.3 Optimal fenestration: maximizing oxygen delivery

We define oxygen concentration to be volumetric, in the sense that  $[O_2]$  is the liters of oxygen per liter of blood and cardiac output  $Q_s$  is defined as liters of blood delivered to the systemic circulation per minute. Thus,  $Q[O_2]$  is the liters of oxygen delivered to the organs per minute and we call this quantity "oxygen delivery".

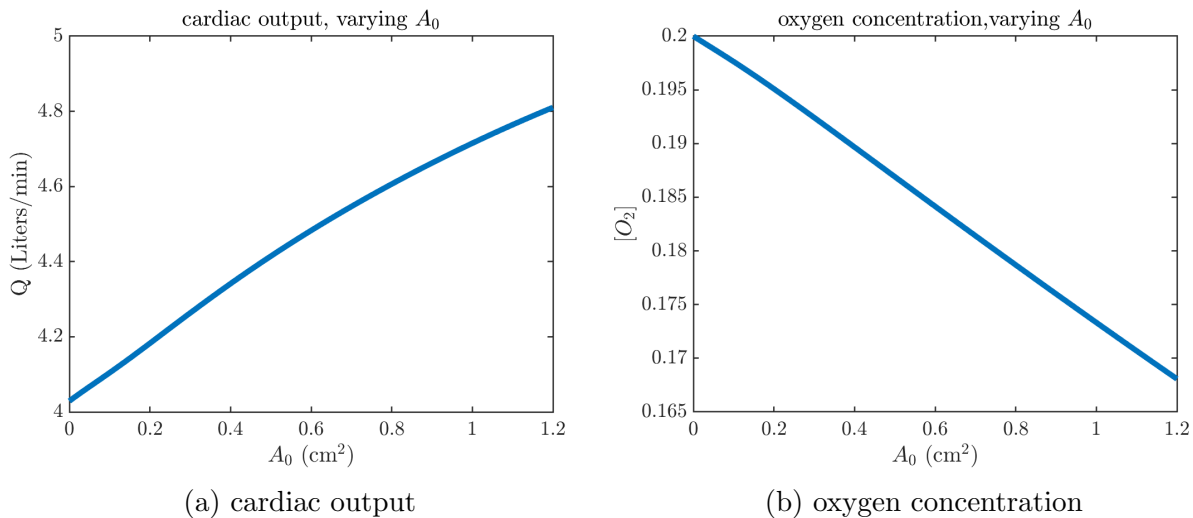


Figure 13: Plots that show the change in cardiac output and systemic arterial oxygen concentration as the fenestration cross sectional area increases.

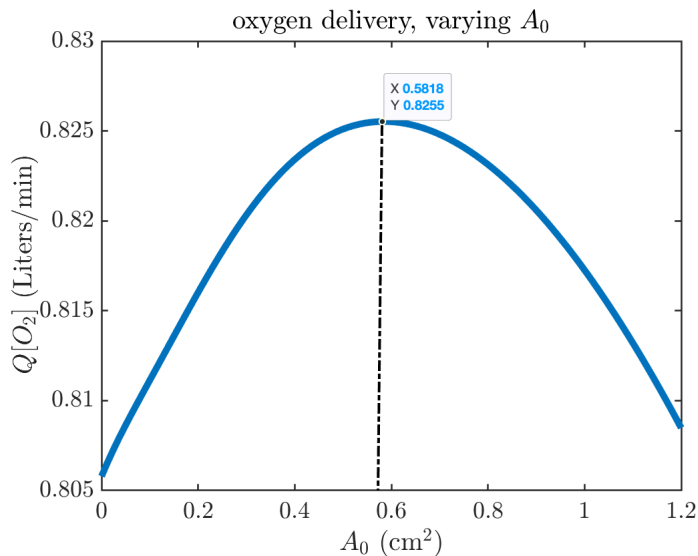


Figure 14: Oxygen delivery ( $Q[O_2]$ ) as a function of fenestration size ( $A_0$ ) with a clear maximum at  $A_0 = 0.5818\text{cm}^2$

variable	closed fenestration	optimal fenestration
cardiac index ( $L \cdot \text{min}^{-1} \cdot \text{m}^{-2}$ )	2.685039	2.979512
stroke volume index ( $\text{mL} \cdot \text{m}^{-2}$ )	42.97555	47.68876
RV end diastolic volume index ( $\text{mL} \cdot \text{m}^{-2}$ )	75.90377	82.01851
RV end systolic volume index ( $\text{mL} \cdot \text{m}^{-2}$ )	32.92821	34.32975
RV end systolic pressure (mmHg)	118.0558	129.8632
RV end diastolic pressure (mmHg)	6.827076	7.556425
vena cava mean pressure (mmHg)	9.348427	9.176109
pulse pressure (mmHg)	56.39481	62.34017
systemic artery systolic pressure (mmHg)	118.0559	129.8023
systemic artery diastolic pressure (mmHg)	61.66108	67.46211
systemic artery mean pressure (mmHg)	93.04392	102.0506
pul artery mean pressure (mmHg)	9.308135	9.149688

Table 4: Calibrated variables from our closed fenestration model compared to those extracted from the optimally fenestrated circulation. Here, the optimal cross-sectional area for the fenestration is  $A_0 = 0.005818 \text{ cm}^2$ . The normalization that occurs in the first four variables assumes a body surface area of  $1.5 \text{ m}^2$ .

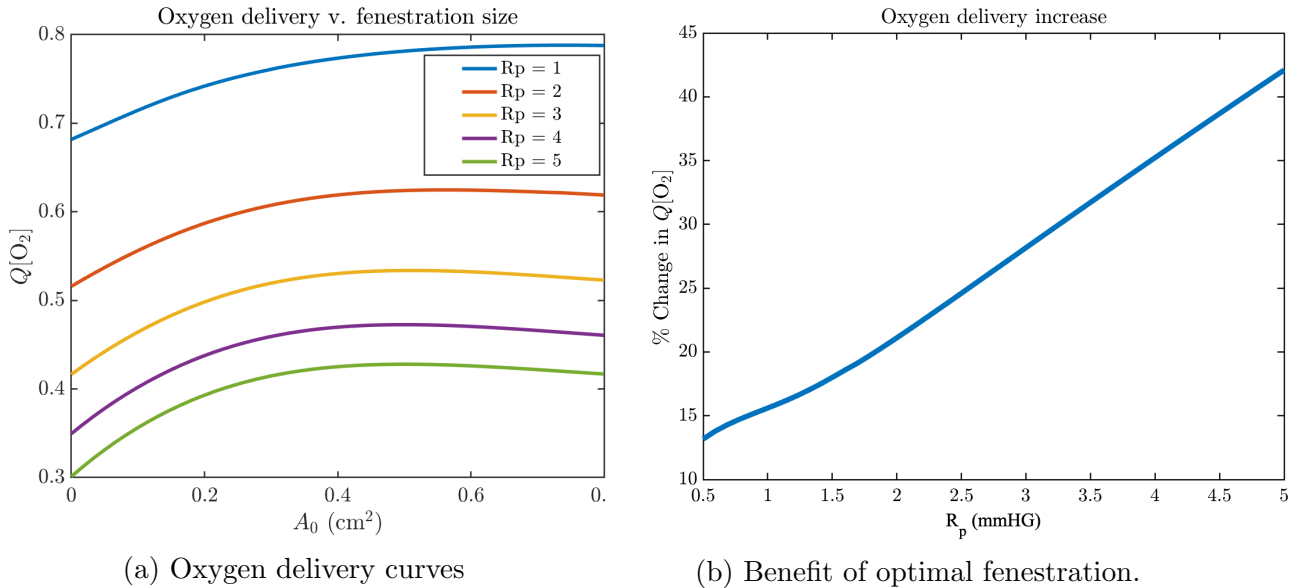


Figure 15: Oxygen delivery curves plotted against fenestration cross-sectional area for varying pulmonary resistance  $R_p$  mmHg/(L/min) values (left). The change in oxygen delivery between the closed fenestration and the optimal fenestration is shown for multiple pulmonary resistance values (right).

## 5 Discussion

After calibrating the standard Fontan circulation with a closed fenestration to clinical data extracted from [5], we can clearly observe that the pressures, flows and oxygen volume had all reached a steady-state by the end of the simulation as seen in figures 5, 6 and 8. The pressure-volume loop shown in figure 7 is for the last cardiac cycle of the simulation. The top left corner of the loop indicates the experimental right-ventricular end-systolic pressure and volume while the bottom right represents the end-diastolic pressure and volume. The blue and red data points correspond to the clinical data from [5] regarding corresponding right-ventricular pressures and volumes at end-systole and end-diastole. The minimum and maximum elastances,  $E_{\min}$  and  $E_{\max}$  were reasonably computed during model calibration to fit these clinical PV data points with  $V_{RVd}$  as an intercept. In the top panel of figure 8, the distribution of oxygen volume across all five chambers is shown and it can be seen that a majority of the circulation's oxygen resides in the organ bed (systemic arteries and systemic veins). In the bottom panel of figure 8 we see the volumetric oxygen concentration after deoxygenation of the blood the the organs (systemic veins and pulmonary arteries) and just after oxygenation from the lungs (pulmonary veins, right ventricle, systemic arteries). These plots justify that the oxygen concentrations that the model fluctuates between as a result of the oxygen source and sink have reached a periodic steady-state at this point in time of the simulation.

Now that we have justified that the oxygen content and the hemodynamics of the closed fenestration model have reached a periodic steady-state and have been calibrated appropriately to clinical data, we can study and compare our results to a model with the fenestration opened.

The right ventricular and systemic arterial pressures are shown in the top and bottom panels respectively in figure 9. Also, as expected, opening the fenestration leads to an increase in the flow through the organ bed and thus cardiac output (see top panel of 10 and 13a). Since the fenestration allows a portion of the blood to be diverted away from the lungs, increasing its cross-sectional area will lead to a decrease in pulmonary flow (bottom panel of figure 10) and a decrease in overall blood oxygen concentration (see figure 15b).

The product of cardiac output (or systemic flow) and oxygen concentration is known as oxygen delivery or the volume of oxygen delivered per minute. Running the simulation for various fenestration sizes to identify the cross-sectional area that results in the maximum value for oxygen delivery allows us to find an optimal balance that helps to increase cardiac output while maintaining as much oxygen concentration as possible. We can visually see this represented in figure 14 where the oxygen delivery as a function of fenestration size results in a parabolic, concave down curve with a clear maximum.

The effects of the optimal fenestration on the circulation are quantitatively represented in table 4 comparing variables of the calibrated closed fenestration simulation to the resulting variables with the optimal fenestration size.

Since a fenestrations are often given to relieve high pulmonary resistances, we wanted to see how varying this parameter affected what fenestration size should be chosen. We found in figure 15a that different pulmonary resistances affect the magnitude of the maximum oxygen delivery value for varying fenestration sizes. It is also clear from figure 15b that for higher pulmonary resistances, the optimal fenestration has a greater impact on improving  $Q[O_2]$ .

## 6 Conclusion

In this paper, we described a model for the standard Fontan physiology in patients with hypoplastic left heart syndrome (HLHS). A clinical procedure that introduces a fenestration from the systemic veins to the pulmonary veins is done to alleviate some of the difficulties that these patients face such as low blood pressure and cardiac output. Our experiments explored a way to optimize the benefits of this fenestration while mitigating some of its adverse effects like loss of blood oxygen content. We operationalized this by studying the effects that varying the fenestration size had on oxygen delivery and found that a clear maximum can be achieved. The optimal fenestration size leads to favorable outcomes regarding cardiac functionality and maintains sufficient blood oxygen concentration in patients with HLHS.

## 7 Appendix A: Steady-state analysis of the fenestrated Fontan circulation

In this section, we derive the steady-state blood flow model. In this case, the compliance of the heart chamber is taken to be constant in time. The compliance of the heart at the end of systole is small, and assumed to be zero corresponding to  $C_{\text{systole}} = 0$ . The compliance of the heart chamber at the end of diastole is denoted  $C_{\text{diastole}}$ .

$$V_{\text{ED}} = V_{\text{d,heart}} + C_{\text{diastole}}P_{\text{pv}}$$

and at end-systole the ventricle achieves its minimum volume given by

$$V_{\text{ES}} = V_{\text{d,heart}} + C_{\text{systole}}P_{\text{pa}}$$

The stroke volume is the volume of blood ejected per beat and is effectively the difference between the end systole:

$$V_{\text{stroke}} = V_{\text{ED}} - V_{\text{ES}} = C_{\text{diastole}}P_{\text{pv}} - C_{\text{systole}}P_{\text{pa}}$$

Taking the heart rate (number of heart beats per minute) to be  $F$ , the cardiac output  $Q$  can then be expressed as:

$$Q = F(V_{\text{stroke}}) = F(C_{\text{diastole}}P_{\text{pv}} - C_{\text{systole}}P_{\text{sa}}) = FC_{\text{diastole}}P_{\text{pv}} = KP_{\text{pv}},$$

where we have defined a pump coefficient  $K = FC_{\text{diastole}}$ . Note that in this model, we are assuming the heart is really just the single ventricle, and the atrium chamber can be effectively lumped with the compliance chamber corresponding to the pulmonary veins. Equations for volumetric flow rate in this model are analogous to Ohm's Law for electrical circuits, with cardiac output behaving as current and pressure difference behaving as voltage difference.

$$\begin{aligned} Q &= KP_{\text{pv}} \\ Q &= R_{\text{s}}^{-1}(P_{\text{sa}} - P_{\text{sv}}) \\ Q - Q_1 &= R_{\text{p}}^{-1}(P_{\text{pa}} - P_{\text{pv}}) \\ Q_1 &= R_{\text{Fe}}^{-1}(P_{\text{sv}} - P_{\text{pv}}) \\ Q - Q_1 &= R_{\text{Fo}}^{-1}(P_{\text{sv}} - P_{\text{pa}}). \end{aligned}$$

The last equation deals with the total cavopulmonary connection in an extracardiac Fontan, and we include the case of both zero and non-zero pressure drops across it. The steady-state assumption being made here is that volume, pressure, and flow are not changing with time. Hence, it must be true that for each compliance chamber, the inflow is equal to the outflow. This is because if the inflow and outflow were unequal, there would be a nonzero change in volume, and we have assumed that the volume in each compliance chamber is constant.

One of our interests is in the dependence of cardiac output  $Q$  on the resistance of the fenestration  $R_{\text{Fe}}$ . To solve for  $Q$ , we first express the pressures as functions of the flows:

$$\begin{aligned} P_{\text{pv}} &= K^{-1}Q \\ P_{\text{pa}} &= R_{\text{p}}(Q - Q_1) + K^{-1}Q \\ P_{\text{sa}} &= QR_{\text{s}} + Q_1R_{\text{Fe}} + K^{-1}Q \\ P_{\text{sv}} &= R_{\text{Fe}}Q_1 + K^{-1}Q \\ P_{\text{Fv}} &= R_{\text{Fo}}(Q - Q_1) + R_{\text{p}}(Q - Q_1) + K^{-1}Q. \end{aligned}$$

From the two equations for  $P_{\text{sv}}$  we get the equality:

$$R_{\text{Fe}}Q_1 = R_{\text{Fo}}(Q - Q_1) + R_{\text{p}}(Q - Q_1),$$

which we can use to express the ratio of fenestration flow to total cardiac output in terms of the pulmonary, fenestration and Fontan resistances:

$$\frac{Q_1}{Q} = \frac{R_{\text{p}} + R_{\text{Fo}}}{R_{\text{Fe}} + R_{\text{p}} + R_{\text{Fo}}}.$$

This relationship can be used to rewrite the pressures in terms of the cardiac output:

$$\begin{aligned} P_{\text{pv}} &= K^{-1}Q \\ P_{\text{sv}} &= \left( \frac{R_{\text{Fe}}(R_{\text{p}} + R_{\text{Fo}})}{R_{\text{Fe}} + R_{\text{p}} + R_{\text{Fo}}} + K^{-1} \right) Q \\ P_{\text{pa}} &= \left( \frac{R_{\text{Fe}}R_{\text{p}}}{R_{\text{Fe}} + R_{\text{p}} + R_{\text{Fo}}} + K^{-1} \right) Q \\ P_{\text{sa}} &= \left( R_{\text{s}} + \frac{R_{\text{Fe}}(R_{\text{p}} + R_{\text{Fo}})}{R_{\text{Fe}} + R_{\text{p}} + R_{\text{Fo}}} + K^{-1} \right) Q. \end{aligned}$$

The volume equations for the compliance chambers are:

$$\begin{aligned} V_{\text{sa}} &= V_{\text{d,sa}} + C_{\text{sa}}P_{\text{sa}} \\ V_{\text{sv}} &= V_{\text{d,sv}} + C_{\text{sv}}P_{\text{sv}} \\ V_{\text{pa}} &= V_{\text{d,pa}} + C_{\text{pa}}P_{\text{pa}} \\ V_{\text{pv}} &= V_{\text{d,pv}} + C_{\text{pv}}P_{\text{pv}}. \end{aligned}$$

We assume the total blood volume in the heart is constant and equal to  $V_0$ , so:

$$\begin{aligned} \sum_i V_i &= V_0 \\ \sum_i C_i P_i &= V_0 - \sum_i V_{\text{d},i} \end{aligned}$$

$$i = \{\text{sa}, \text{sv}, \text{pa}, \text{pv}\}$$

Next we define three time constants,  $T_1, T_2, T_3$ , as follows:

$$\begin{aligned} T_1 &= K^{-1} \sum_i C_i + C_{\text{sa}} R_{\text{s}} \\ T_2 &= (C_{\text{sa}} + C_{\text{sv}} + C_{\text{pa}}) R_{\text{p}} \\ T_3 &= (C_{\text{sa}} + C_{\text{sv}}) R_{\text{Fo}} \end{aligned}$$

Finally, we use the equation for volume conservation to express  $Q$  as a function of  $R_{\text{Fe}}$ :

$$Q = \left( T_1 + (T_2 + T_3) \frac{R_{\text{Fe}}}{R_{\text{Fe}} + R_{\text{p}} + R_{\text{Fo}}} \right)^{-1} (V_0 - \sum_i V_{d,i})$$

where  $T_1, T_2$ , and  $T_3$  are expressions only containing model parameters. This function is visualized in the left panel of Figure 16. In the right panel we plot pressures in the different compliance chambers to see if the parameters in our model are calibrated in a reasonable way.

The cardiac output  $Q = Q(R_{\text{Fe}})$  as a function of the fenestration resistance is monotone decreasing, i.e. as  $R_{\text{Fe}}$  increases, the cardiac output decreases. In particular, this formula shows that an open fenestration corresponding to  $R_{\text{Fe}} < \infty$  will give higher cardiac output than a closed fenestration corresponding to  $R_{\text{Fe}} = \infty$ .

We can also investigate the effect of the fenestration on the systemic venous pressure. To do this, define the following function of  $R_{\text{Fe}}$ :

$$\gamma(R_{\text{Fe}}) = \frac{R_{\text{Fe}}}{R_{\text{Fe}} + R_{\text{p}} + R_{\text{Fo}}},$$

which takes values between 0 and 1 for  $0 < R_{\text{Fe}} < \infty$ . We can then express the systemic venous pressure in terms of  $\gamma$ :

$$P_{\text{sv}} = \frac{(\gamma(R_{\text{p}} + R_{\text{Fo}}) + K^{-1})(V_0 - \sum_i V_{d,i})}{T_1 + (T_2 + T_3)\gamma}.$$

Differentiating this equation with respect to  $\gamma$ , we obtain:

$$\frac{dP_{\text{sv}}}{d\gamma} = \frac{[(T_1 + \gamma(T_2 + T_3))(R_{\text{p}} + R_{\text{Fo}}) - (\gamma(R_{\text{p}} + R_{\text{Fo}}) + K^{-1})(T_2 + T_3)](V_0 - \sum_i V_{d,i})}{(T_1 + \gamma(T_2 + T_3))^2}.$$

Cancelling terms gives us:

$$\frac{dP_{\text{sv}}}{d\gamma} = \frac{(T_1(R_{\text{p}} + R_{\text{Fo}}) - (T_2 + T_3)K^{-1})(V_0 - \sum_i V_{d,i})}{(T_1 + \gamma(T_2 + T_3))^2} > 0,$$

which follows since  $T_1(R_{\text{p}} + R_{\text{Fo}}) > (T_2 + T_3)K^{-1}$ . So, we conclude that opening a fenestration in this model *always* leads to a drop in the systemic venous pressure.

Each compliance chamber has an oxygen concentration  $[O_2]$ , and we are interested in  $[O_2]_{sa}$  as a function of the fenestration resistance. We assume the concentration in the pulmonary veins is given,

$$[O_2]_{pv} = C^* = 0.2.$$

Also, we know the concentration in the systemic veins and pulmonary arteries is the same because of the Fontan connection:

$$[O_2]_{sv} = [O_2]_{pa}.$$

Assume the systemic organs consume oxygen at a rate  $M$ . By the Fick principle:

$$Q[O_2]_{sa} - Q[O_2]_{sv} = M.$$

The final equation is conservation of oxygen at the junction where the fenestration connects to the pulmonary veins:

$$Q_1[O_2]_{sv} + (Q - Q_1)[O_2]_{pv} = Q[O_2]_{sa}.$$

These equations for oxygen can be simplified to express:

$$[O_2]_{sa} = C^* - \left(1 - \frac{Q_1}{Q}\right)^{-1} \frac{Q_1}{Q} \frac{M}{Q}.$$

Using the relationship between fenestration flow and cardiac output, this formula can be rewritten as:

$$[O_2]_{sa} = C^* - \frac{M R_p + R_{Fo}}{Q R_{Fe}},$$

revealing that systemic arterial oxygen delivery,  $A_{O_2}$ , can be expressed as a function of the fenestration resistance in the following way:

$$A_{O_2} = Q[O_2]_{sa} = QC^* - M \frac{R_p + R_{Fo}}{R_{Fe}}.$$

In the formula above, note the cardiac output  $Q$  is also a function of  $R_{Fe}$  as described in the previous section. When the fenestration is closed,  $R_{Fe} = \infty$ , and we obtain  $A_{O_2} = QC^*$  as expected. Otherwise, the fenestration is open and has some impact on oxygen delivery.

An important question is if there is a choice of  $R_{Fe}$  for which  $A_{O_2}$  is maximized. In Figure 17, we plot  $A_{O_2}$  for different values of oxygen consumption  $M$  on the left and different values of the lung resistance  $R_p$  on the right. All the figures reach some maximum value of oxygen delivery.

Assuming a maximum for  $A_{O_2}$  exists, we can derive conditions under which

$$\frac{dA_{O_2}}{dR_{Fe}} = 0.$$

We have

$$\begin{aligned}\frac{dA_{O_2}}{dR_{Fe}} &= C^* \frac{dQ}{dR_{Fe}} + M \frac{R_p + R_{Fo}}{R_{Fe}^2}, \\ \frac{dQ}{dR_{Fe}} &= \frac{(V_0 + \sum_i V_{d,i})(T_2 + T_3)(R_p + R_{Fo})}{(T_1(R_p + R_{Fe} + R_{Fo}) + (T_2 + T_3)R_{Fe})^2}.\end{aligned}$$

Introducing the notation  $x = (R_p + R_{Fo})/R_{Fe}$ , we have

$$\frac{dA_{O_2}}{dR_{Fe}} = 0 \iff M((x+1)T_1 + T_2 + T_3)^2 = C^*(V_0 - \sum_i V_{d,i})(T_2 + T_3).$$

Solving the quadratic equation, we obtain:

$$x_{\pm} = \frac{-T_1 - (T_2 + T_3) \pm \left( \frac{C^*(V_0 - \sum_i V_{d,i})(T_2 + T_3)}{M} \right)^{1/2}}{T_1}$$

There is only one root which has the chance of being positive, corresponding to a fenestration resistance  $R_{Fe}^*$ :

$$\frac{R_p + R_{Fo}}{R_{Fe}^*} = \frac{-T_1 - (T_2 + T_3) + \left( \frac{C^*(V_0 - \sum_i V_{d,i})(T_2 + T_3)}{M} \right)^{1/2}}{T_1},$$

which we rewrite as

$$R_{Fe}^* = \frac{T_1(R_p + R_{Fo})}{-T_1 - (T_2 + T_3) + \left( \frac{C^*(V_0 - \sum_i V_{d,i})(T_2 + T_3)}{M} \right)^{1/2}}.$$

In particular, this fenestration resistance is positive if and only if

$$C^*(V_0 - \sum_i V_{d,i}) > M(T_2 + T_3) \left( \frac{T_1 + T_2 + T_3}{T_2 + T_3} \right)^2.$$

## 7.1 Steady-state results

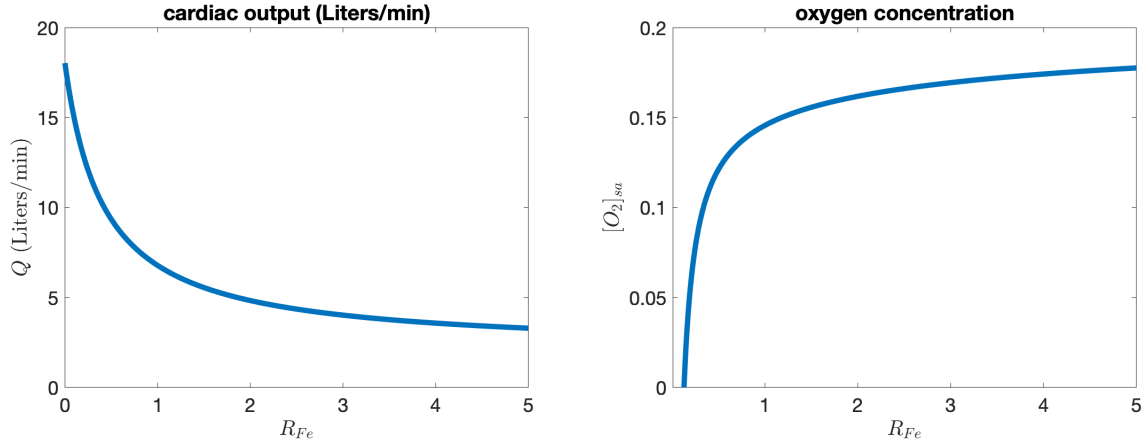


Figure 16: Cardiac output  $Q$  on the left oxygen concentration as a function of the fenestration resistance on the right. As  $R_{Fe} \rightarrow \infty$ , the oxygen concentration approaches 0.2.

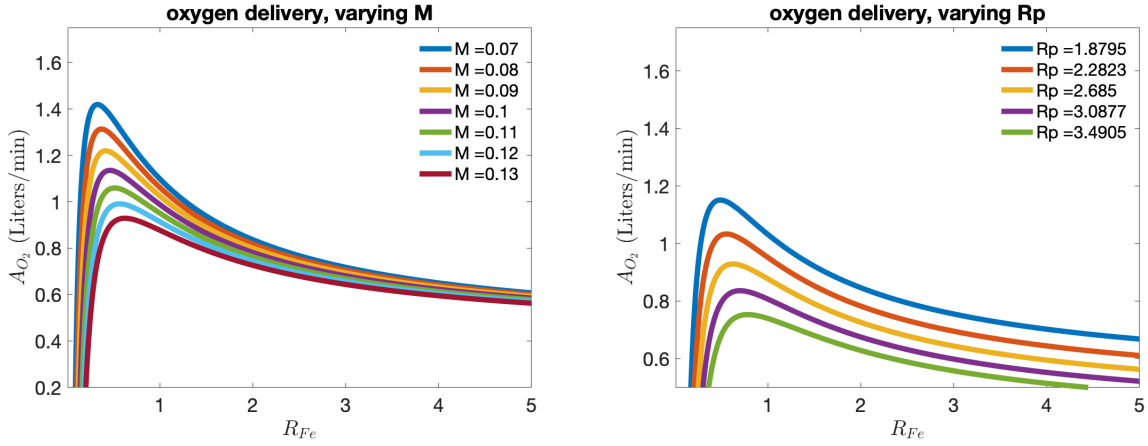


Figure 17: Systemic arterial oxygen delivery as a function of the fenestration resistance  $R_{Fe}$ . On the left we vary  $M$ , the rate of oxygen consumption in the organs, and on the right we vary  $R_p$ , the resistance of the lungs.

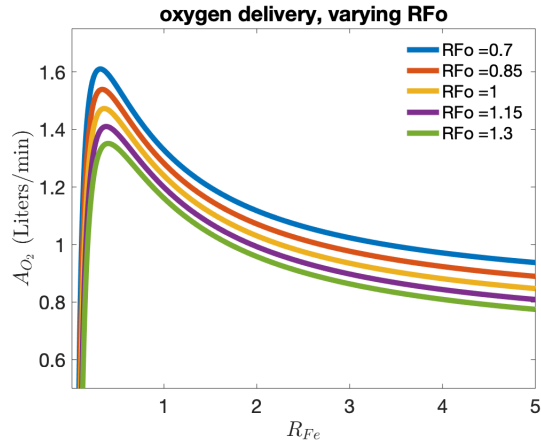


Figure 18: This figure shows the oxygen delivery curves for different values of  $R_{Fo}$ , resistance of the Fontan connection.

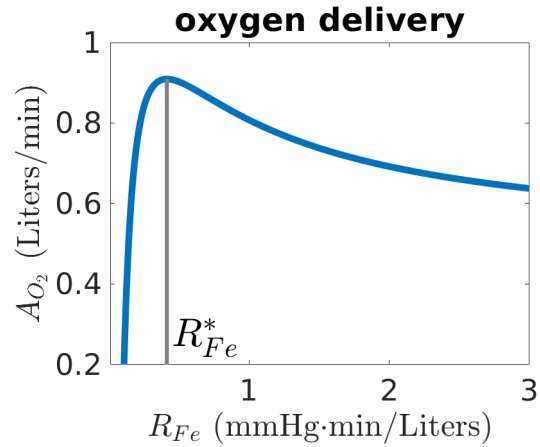


Figure 19: This figure closely shows that an optimal fenestration resistance can be identified to maximize oxygen delivery to the systemic circulation in a fenestrated Fontan circulation.

## 7.2 Square law fenestration resistance

Our goal in this section is to relate the fenestration resistance to geometric parameters. A place to start would be to assume that the fenestration is a square law resistor:

$$P_{sv} - P_{pv} = \frac{\rho}{2} \left( \frac{Q_1}{A} \right)^2,$$

where  $A$  is defined to be the cross sectional area of the fenestration. Using the equations above we get the following formulas for the systemic venous and pulmonary artery pressures:

$$\begin{aligned} P_{sv} &= \frac{\rho}{2} \left( \frac{Q_1}{A} \right)^2 + K^{-1}Q \\ P_{pa} &= R_p(Q - Q_1) + K^{-1}Q. \end{aligned}$$

Given our model assumption that  $P_{sv} = P_{pa}$ , we get a quadratic equation for  $Q_1$ :

$$\frac{\rho}{2} \left( \frac{Q_1}{A} \right)^2 = (Q - Q_1) \iff Q_1^2 + \beta Q_1 - \beta Q = 0,$$

with  $\beta = \frac{2R_p A^2}{\rho}$ . The only positive root of this equation is

$$Q_1 = Q_1(Q) = -\frac{\beta}{2} + \frac{1}{2} (\beta^2 + 4\beta Q)^{1/2}.$$

Using the equation:

$$C_{sa}P_{sa} + (C_{sv} + C_{pa})P_{sv} + C_{pv}P_{pv} = V_0,$$

with  $P_{sa} - P_{sv} = R_s Q$ , we obtain a nonlinear equation for the cardiac output  $Q$  as a function of the parameters:

$$\begin{aligned} C_{sa}R_s Q + (C_{sa} + C_{sv} + C_{pa})P_{sv} + C_{pv}K^{-1}Q &= V_0 \\ P_{sv} &= \frac{\rho}{2} \left( \frac{Q_1}{A} \right)^2 + K^{-1}Q \\ Q_1 &= -\frac{\beta}{2} + \frac{1}{2} (\beta^2 + 4\beta Q)^{1/2}. \end{aligned}$$

## References

- [1] F Fontan and E Baudet. Surgical repair of tricuspid atresia. *Thorax*, 26(3):240–248, 1971.
- [2] Mark K Friedberg and Andrew N Redington. Right versus left ventricular failure: differences, similarities, and interactions. *Circulation*, 129(9):1033–1044, 2014.
- [3] Marc Gewillig and Stephen C Brown. The fontan circulation after 45 years: update in physiology. *Heart*, 102(14):1081–1086, 2016.
- [4] Frank C Hoppensteadt and Charles S Peskin. *Mathematics in Medicine and the Life Sciences*, volume 10. Springer Science & Business Media, 2013.
- [5] Matthew Jolley, Steven D Colan, Jonathan Rhodes, and James DiNardo. Fontan physiology revisited. *Anesthesia & Analgesia*, 121(1):172–182, 2015.
- [6] Luc Mertens, Donald J Hagler, Ursula Sauer, Jane Somerville, and Marc Gewillig. Protein-losing enteropathy after the fontan operation: an international multicenter study. *The Journal of thoracic and cardiovascular surgery*, 115(5):1063–1073, 1998.
- [7] JP Mynard, MR Davidson, DJ Penny, and JJ2946553 Smolich. A simple, versatile valve model for use in lumped parameter and one-dimensional cardiovascular models. *International journal for numerical methods in biomedical engineering*, 28(6-7):626–641, 2012.
- [8] Charles Puelz, Sebastián Acosta, Béatrice Rivière, Daniel J Penny, Ken M Brady, and Craig G Rusin. A computational study of the fontan circulation with fenestration or hepatic vein exclusion. *Computers in biology and medicine*, 89:405–418, 2017.